A PHOSPHORESCENT THERMAL HISTORY SENSOR

A. Rabhiou[*]   *J. Feist*[+]   *A. Kempf*[*]   *A. Heyes* [*, 1]

[*]Mechanical Engineering Department, Imperial College, London, UK
[+]Southside Thermal Sciences (STS) Ltd., Imperial Innovations, Imperial College, London, UK

ABSTRACT
Engine components exposed to harsh combustion conditions are often not accessible for on-line temperature monitoring. The temperature of the surface of these components can be measured off-line, by sensors that record their thermal history. Thermal paints are an example of this type of sensor, but have many disadvantages. Alternatively, phosphor coatings can be used as thermal history sensors. These undergo permanent changes when exposed to elevated temperatures, which affect their emission characteristics. The coatings can be interrogated after the exposure and reveal their thermal history. In this paper, an experimental investigation of the phase change of $Y_2O_2S : Eu$ is reported and used as a phosphorescent thermal history sensor. The phosphor powder was annealed at different temperatures, and characterised using photo-luminescence spectroscopy.

NOMENCLATURE
PMT photomultiplier tube
CCD charge coupled device
XRD X-ray diffraction
REACH Registration, Evaluation, Authorisation and Restriction of Chemical substances
CRT cathode ray tube
CTS charge transfer state
UV ultra-violet
RGB Red-Green-Blue
HSV Hue-Saturation-Value
FWHM full width at half maximum

INTRODUCTION
Many engineering components must operate in a high temperature environment. This is particularly true in gas turbines, where components are exposed to hot gas streams whose temperature may exceed the material limits. The excessive temperatures can degrade the mechanical properties of these components. As part of the design process, it is necessary to predict the thermal history of the surface of these components. Measuring thermal history in a non-destructive fashion is not trivial. The harsh environment of combustion also requires robust instrumentation. On-line in-situ measurements are not always possible due to limited access to the surfaces of concern. Under these circumstances, it is highly desirable to have a robust, non-intrusive sensor that can be placed in or on the relevant components and record the temperatures to which they are exposed, in such a way that it can be read-out later off-line. Such sensors are sometimes referred to as *thermal history sensors* due to their ability to *remember* the temperature to which they have been exposed.

Thermal paint
Probably the best known type of thermal history sensor are thermal paints, that are widely used in gas turbine development [Watson and Hodgkinson, 2002]. Active ingredients are metallic compo-

---

[1]Corresponding author: a.heyes@imperial.ac.uk

nents, which are suspended in a binder or resin. The metallic components cause the paint to change colour depending on the temperature and duration of the exposure. The thermally activated chemical reactions of these metallic components alter their chemical bonds with molecules such as water, carbon dioxide or ammonia [Neely and Tjong, 2008]. This results in permanent changes in the reflection spectra of the metallic components [Cowling et al., 1953, Lempereur et al., 2008]. Different metallic components will have different colour changes, and thus different thermal responses. The paints are usually applied as a thin layer ($\sim 25 \ \mu$m). The engine is then run for a defined period (generally 5 to 10 min), stopped and disassembled in order to analyse the changes in colour.

Thermal paints have been a valuable tool of engine developers for many years, but the existing paints present a number of challenges if reliable results are to be obtained. Calibrated colour charts must be used by an experienced, trained and certified operator to interpret the colour changes and to draw isothermal lines directly onto the components. The colour changes are often subtle; the operator can only detect a few discrete temperature values, where sharp colour changes occur. At these temperatures, the resolution is around 10 °C at best. Most paints however have large temperature ranges over which the colour changes cannot be discriminated, which results in poor resolution [Bird et al., 1998]. The gathered temperature data is somewhat subjective and dependent on local conditions, such as ambient lighting, which must be carefully controlled.

Efforts have been made to automate interpretation of the colour changes, using colour models, such as RGB (Red-Green-Blue) or HSV (Hue-Saturation-Value) [Lempereur et al., 2008, Smith, 2002]. The HSV is a geometrical representation of colours that is based on intensity, lightness and position within the reflectance spectrum. Colours are thus characterised by multiple parameters, which complicates interpretation and calibration of colour changes. Lighting conditions and observation distances and angles are critical for reproducible and accurate measurements [Lempereur et al., 2008].

Automation efforts conducted so far have not been completely successful in removing ambiguity and offering a substitute for the human operator. They also increase the cost and complexity of the technique. The difficulty of performing temperature read-outs in-situ and the consequent requirement to strip down the engine and examine components under laboratory conditions is another problem. Even where optical access is available, by use of a boroscope, reading out colour changes is not yet possible, with a particular difficulty being the achievement of homogeneous illumination of the surface inside an engine [Bird et al., 1998].

Some thermal paints contain components that are hazardous, such as chromium, lead and nickel cobalt [Watson and Hodgkinson, 2003]. The European Commission introduced REACH (Registration, Evaluation, Authorisation and Restriction of Chemical substances) legislation in 2007 that requires companies to seek for alternatives to hazardous materials [Regulation EC, 12.2006]. Other thermal paints contain expensive noble metals such as gold, silver, bismuth and platinum, adding significantly to the cost of their use [Rolls-Royce, 1988].

The review above indicates the value of thermal history sensors and the utility of existing thermal paints, but also suggests how existing paints and read-out systems could be improved. Specifically, an ideal thermal history sensor would be low cost, non-toxic, have a wide dynamic range and continuous variation in the measurement, a good temperature resolution and would permit automated reading via electronic imaging with the possibility of doing so in-situ, ideally using a boroscope.

Alternative Thermal History Sensors

Fair et al. [2008] have proposed a thermal history sensor based on a glass-ceramic array which crystallises due to thermal exposure. The glass-ceramics, made of alkali or transition metal alumino-silicates, are melted and quenched on substrates. When exposed to high temperatures, they undergo nucleation and crystallite growth. The transmittance of the material, which decreases with increasing exposed temperature and time, is used as indicator of the thermal history. However, an elaborate cal-

ibration database is required, illumination and observation angles must be controlled, and resolution is poor ($\sim 50\,°C$). The transmittance can be the same for different exposure regimes, and mechanical strain on the sensor can have a similar effect on the transmittance - both introduce ambiguity.

Nikolaenko et al. [1976] have designed at the Kurchatov Institute a measuring device, called IMTK, based on the dependency of the lattice parameter of diamond or silicon carbide, irradiated by neutrons, on the annealing temperature and time. Neutron irradiation causes point defects, vacancies and interstitials in the crystal lattice. The point defects causes the crystal lattice to swell. The annealing process annihilates the interstitials and vacancies and causes a decrease of the lattice swelling. Using X-ray diffraction (XRD) and knowing the annealing time, the annealing temperature can be obtained. The temperature range offered extends from 150 to 1400 $°C$, with an average measurement error of 15 $°C$. The crystals are encapsulated in a metal container, which is adhered to the surface of the object of interest Volinsky et al. [2005]. The adherence and the subsequent intrusive character of the sensor is a disadvantage for use on the inner surface of a gas turbine. This sensor only allows for point measurements, and requires an exact knowledge of the annealing path, as time has a major influence on the results. The readout is done using XRD, which can only be done in laboratory conditions, so that in situ measurements are not feasible.

Feist et al. [2007] have proposed a thermal history sensor based on phosphors that undergo permanent changes in their light emission properties when exposed to high temperatures. Non-permanent changes in thermographic phosphors have been used for many years to measure surface temperatures or heat fluxes under conditions relevant to gas turbines [Allison and Gillies, 1997, Brubach et al., 2008, Feist et al., 1999, Heyes et al., 2008, Steenbakker et al., 2009]. The emission properties of these phosphors are reversible, so that on-line measurements can be made. However, there are temperature driven processes associated with other phosphors that lead to irreversible changes in their emission characteristics. These processes are reported in the literature on optimising output from the phosphors or on conditions under which they will cease to phosphoresce. As far as the current authors are aware, there has been no previous attempt to utilise these permanent changes for the purpose of temperature measurements.

The proposed phosphorescent thermal history sensor, presented in this work, has the advantage over thermal paints of undergoing irreversible changes which are reflected in the emission properties. These are easily and unambiguously measurable with standard spectroscopic instrumentation. The spectra have sharp and clearly defined emission lines, so that changes in the emission can be quantitatively measured by analysis of the spectrum. This will allow for relatively easy automation of the readout and, thus, to more objective read-outs. In addition, in-situ interrogation of the sensor should be possible.

The present paper is structured as follows. An introduction to the relevant theory of luminescence is presented. The concept of phosphor based thermal paints is then discussed. Different physical processes causing irreversible changes in phosphorescence are described and categorized. The paper then describes an experimental demonstration, based on phase changes in $Y_2O_2S : Eu$. Calibration curves of this phosphor are presented and discussed.

INTRODUCTION TO LUMINESCENCE OF PHOSPHORS

Phosphors are synthetic ceramic materials with a high melting point - often exceeding 2000 $°C$. They comprise a host, doped with small quantities of rare earth or transition metal ions as the optically active component. Phosphors absorb UV-light, which promotes electrons to excited levels, and the electrons eventually fall back to their ground levels through radiative and non-radiative transitions. Radiative transitions are referred to as luminescence. Non-radiative transitions involve the emission of phonons, which are vibrations releasing the excited electron energy through heat.

The rate of depopulation of an excited level *e* to the ground level *g* is described by following

equation:

$$\frac{dN_e}{dt} = -N_e \cdot P_{e \to g}, \tag{1}$$

where $P_{e \to g}$ is the transition probability of radiative and non-radiative decays, N_e is the density of excited centres and t is the time. The solution to equation (1), assuming the emission intensity to be directly proportional to the excited electron population, gives the intensity of the emitted light I at time t:

$$I(t) = I(0) \cdot e^{-\frac{t}{\tau}}, \tag{2}$$

The emission lifetime decay τ is the inverse of the sum of the radiative P_r and non-radiative P_{nr} decay transition probabilities:

$$\tau = (P_r + P_{nr})^{-1} \tag{3}$$

Commonly used dopants are europium (Eu) [Rabhiou et al., 2009], terbium (Tb) [Chambers and Clarke, 2007], dysprosium (Dy) [Heyes et al., 2008] and manganese (Mn) [Brubach et al., 2008]. They are optically active, and favour radiative transitions directly back to the ground state, so they are efficient bright emitters. Rare-earth ions in their trivalent valence state (e.g. Eu^{3+}) have very narrow emission lines because the electrons associated with the emission transitions are shielded from the influences of the host.

Figure 1 shows the energy level diagram of Eu^{3+} and the different luminescence processes taking place. The energy transitions were calculated from the Dieke diagram [Dieke et al., 1968]. Laser illumination promotes electrons to excited energy levels. At room temperature, the radiative transitions from excited energy levels $^5D_3$, $^5D_2$ and $^5D_1$ are usually quenched, in favour of $^5D_0$. From this excited level, several radiative transitions bring the electrons back to their ground states. This decays results in narrow, bright emission lines.

The emission is not immune from the effects of temperature, however, it is rather that changing temperature affects the emission spectrum in very distinct ways that are easy to assess in an automated fashion. This is making phosphors an ideal material for objective temperature measurements.

PHOSPHORESCENT THERMAL HISTORY SENSOR'S CONCEPT

The concept of a phosphorescent thermal history sensor is based on phosphors that undergo irreversible changes that are reflected in their emission properties when exposed to high temperatures. These changes may be manifest in the lifetime decay, the emission intensity or a shift in the emission lines of the spectrum. All these parameters can be observed individually and can reveal the thermal history of the exposure of the phosphor. In other words, with proper calibration, the maximum operating temperatures can be *remembered* by the phosphor.

Thanks to the intense and sharp emission lines in the spectra of phosphors, a sensitive photomultiplier tube (PMT) can be focused on a peak wavelength and record both intensity and lifetime decay. The emission spectra of phosphors are brighter than the reflectance spectra from coloured surfaces, which results in a better signal-to-noise ratio under automated/machine reading conditions. The influence of lighting condition, angle of observation and dirt deposition on the surface on the emission intensity can be removed, by incorporating into the paint a reference phosphor that is fully stable and does not change its emission properties during annealing, as proposed by Feist et al. [2007]. The ratio of the emission from both components will cancel these effects, leaving only the influence of temperature. The lifetime decay on the other hand is automatically independent of these factors, and offers another robust measurement variable.
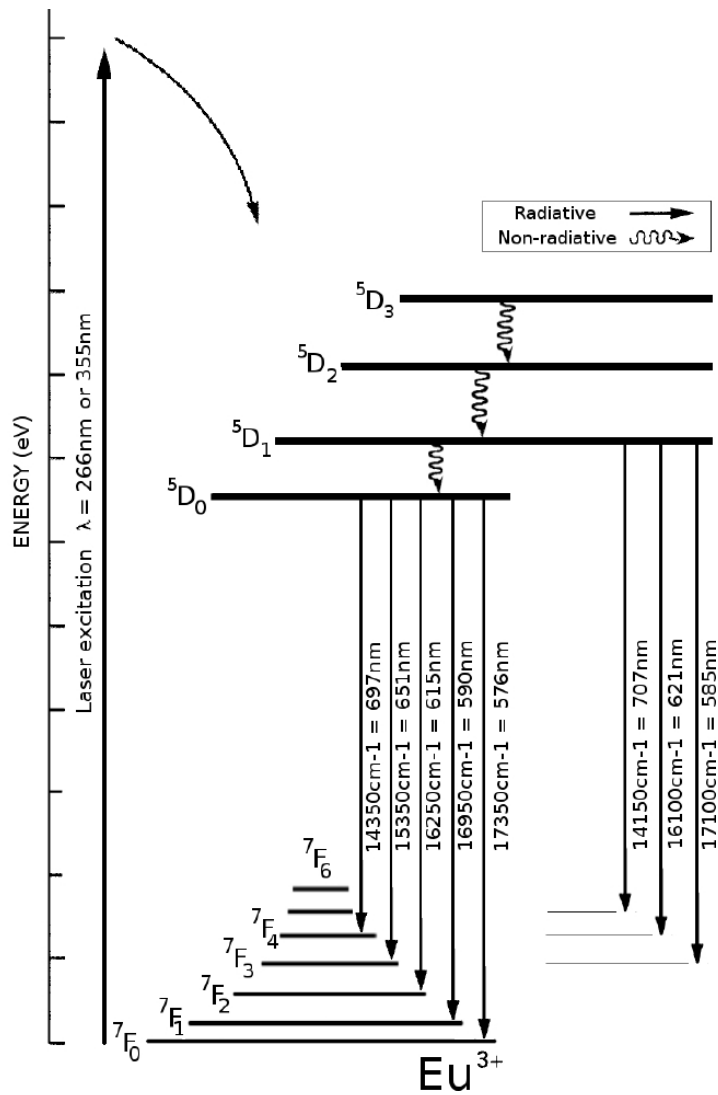
Figure 1: **Energy diagram and main luminescence processes of** Eu^{3+}

Longer exposures at lower temperatures could result in similar changes, so control over the exposure time must be maintained or additional calibration carried out. This feature of a phosphorescent thermal sensor is shared with classical thermal paints [Lempereur et al., 2008]. However, the thermal exposure period for thermal paints is often very short (5 to 10 min) - to achieve good results. Longer engine tests do not guarantee high resolution of thermal paints [Bird et al., 1998]. Phosphorescent thermal history paints will be less costly and hazardous than thermal paints, as the phosphor based paints do not contain expensive metals nor toxic elements.

A requirement for a candidate phosphor is a continuous change in its luminescent properties over the desired dynamic temperature range (e.g. between 600 and 1300 °C). After the exposure to high temperatures, the luminescence must be observable and measurable. Another requirement is chemical stability; the phosphor must not react with the environment, unlike some existing thermal paints which are affected by gas composition [Bird et al., 1998].

Three different processes have been identified which can cause thermally driven permanent emission changes as a result of high temperature exposure [Feist et al., 2007]. These different categories are discussed in detail below, and examples from the literature are given. Their potential as thermal history sensors is also discussed.

Amorphous-to-Crystalline Process

Phosphors in an amorphous state usually do not emit or have very weak and broadband emission. The excitation spectrum is much broader than in fully crystalline phosphors [Zhou et al., 2002]. In the amorphous state, the vicinity of each dopant ion is different and thus has a different excitation and emission energy. The observed emission is the sum of the individual emissions of a large number of ions and hence amorphous materials tend to have broad lines in their emission and excitation spectra.

The emission intensity and the lifetime decay often increase when a phosphor changes from amorphous to crystalline. This process takes place at elevated calcination temperatures, where impurities such as OH^-, H_2O, NO_3^- and CH_2^-, present in the amorphous phosphor, evaporate. These impurities are very efficient quenchers of luminescence. As their concentration decreases, the non-radiative transition probability decreases and thus the lifetime decay increases. With increasing calcination temperatures, the host crystallises and the dopants are integrated into the crystal structure of the phosphor. This so-called activation of the dopant ions results in increased emission and sharpened emission lines.

Examples of amorphous-to-crystalline changes in phosphors in the literature are abundant. Zhang et al. [2002] have calcined amorphous $Y_2O_3 : Eu$ particles and observed an increase of the emission intensity from 600 to 1300 °C. Zhou and Lin [2005] have crystallised $YVO_4 : Eu$ particles and reported an increase of the emission intensity from 500 to 1100 °C.

Phase-Change Process

Some phosphors undergo post-crystallisation changes in their emission properties when exposed to high temperature. This can be due to phase changes and the emission spectra can change radically, as is the case for oxysulfides [Poston et al., 2003, Feist and Heyes, 2000, 2001]. The thermal decomposition of such materials is a well-known and important metallurgical and chemical reaction. Sulphur evaporates at high temperature, and a sulphur free phase appears in the material. The ions within this sulphur-free phase are bound to the crystal differently and this influences the emission spectrum.

Diffusion of Dopants, Quenchers or Sensitizers into Host

The diffusion of dopants in an undoped host is time and temperature dependent and both the lifetime and emission decay are dependent on the level of dopant concentration. Also, a phosphor's emission efficiency can be improved by adding small amounts of particular rare earth or transition metal ions to it. In the literature, this secondary dopant is called a sensitiser [Blasse and Grabmaier, 1994]. Some phosphors have long decay times, and extra dopant ions are added to reduce the lifetime decay to suit a particular application. In this case the additional ion is called a quencher. Sometimes the quenching is undesired, in which case the responsible ions are termed impurities or killers.

These processes are all very similar. The diffusion of the ions within the phosphor either activates luminescence, facilitates non-radiative transitions, or improves energy transitions between the energy receiver and the emitting ions. These processes can be used for the purpose of thermal history sensing, since the process of diffusion of ions in a host is time and temperature dependent.

DEMONSTRATION OF PHASE CHANGE PROCESS

In this paper, an experimental demonstration of the phase-change process is given. For this purpose we use the phosphor $Y_2O_2S : Eu$, which is an important red-emitting phosphor for cathode-ray tubes (CRTs) and lighting. It has a very high luminous efficiency and its emission is thus very bright.

Figure 2 shows the excitation and emission spectra of $Y_2O_2S : Eu$. The excitation spectrum is very broadband. A first band, around 260 nm, characterises the excitation of the host. The host then passes the energy to the dopants. The second band, around 340 nm, characterises the excitation of the
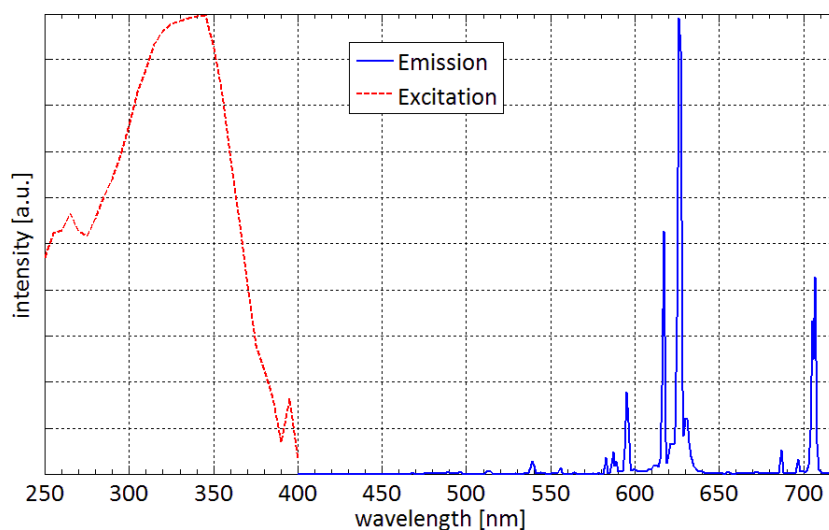
Figure 2: **Excitation [Phosphor Technology Ltd] and emission spectra of** $Y_2O_2S : Eu$

charge transfer states (CTS). The emission spectrum in figure 2, shows narrow emission lines between 580 and 710 nm. All these emission lines are a result of optically forbidden $4f - 4f$ transitions. Emission lines from higher excited states ${}^5D_3, {}^5D_2$ and ${}^5D_1$ are quenched in favour of transition for the ${}^5D_0$ excited state. The weak emission line at 583 nm corresponds to the ${}^5D_0 \rightarrow {}^7F_1$ transition of Eu^{3+} ions. The emission peaks at 616 and 626 nm are strong and originate from transition ${}^5D_0 \rightarrow {}^7F_2$. The emission peak at 705 nm is due to the ${}^5D_0 \rightarrow {}^7F_4$ transition [Fonger and Struck, 1970].

The phosphor was annealed at different temperatures, between 700 and 1400 °C. Alumina crucibles were filled with around 3 g of the phosphor and placed inside a box-furnace (Lenton Furnace) for 20 and 40 min, in air at ambient pressure. The phosphor powder samples were examined at room temperature after the heat-treatment process. The samples were excited using a pulsed Nd:YAG laser (Spectra Physics) emitting at 266 and 355 nm. The laser has a repetition rate of 10 Hz, a pulse width of 5 to 7 ns and a maximum pulse energy of 110 and 220 mJ, at 266 and 355 nm respectively (See figure 3).
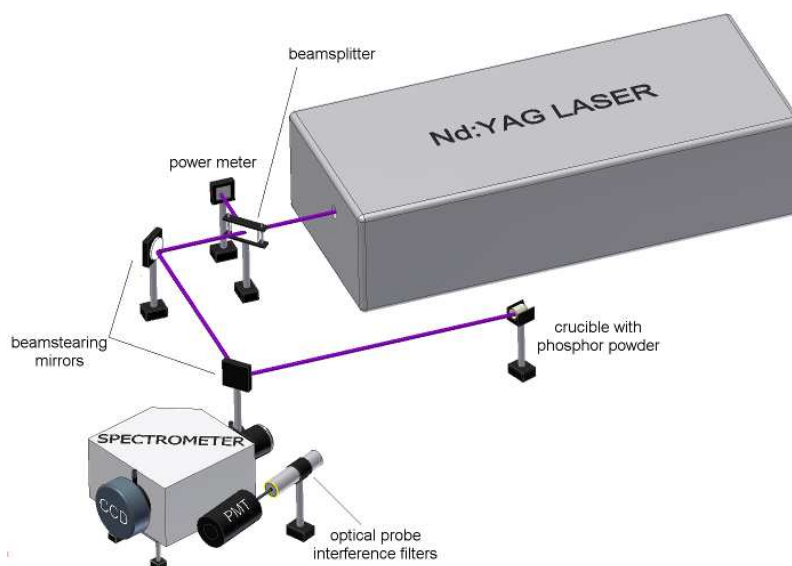

Figure 3: **Experimental set-up for phosphorescence calibration**

For the emission spectra, the luminescence was captured using a 50 mm Nikon lens, which focused the emission onto the entrance slit (50 μm) of a crossed Czerny-Turner spectrometer (HoribaJobin Yvon MicroHR). At the exit, a pre-calibrated CCD linear array measured the intensities and spectral position of emission lines, with an exposure time of 0.4 s. The wavelength resolution was smaller than 0.2 nm. For the lifetime decay measurements, the emission was captured with a optical probe, with a high acceptance angle, which collects and couples the light into a fiber bundle. The latter is coupled to a PMT via narrowband interference filters at 610 and 630 nm (FWHM = 10 nm). A single exponential was fitted to the data using a commercial Levenberg-Marquardt least-square algorithm.

Results and Discussion

Photoluminescent Spectra

Figure 4 shows the emission spectrum of $Y_2O_2S : Eu$ phosphor particles around 611 and 705 nm, annealed for 40 min, as a function of the annealing temperature. The phosphor was excited at 266 nm, which triggers the host absorption. One can see that the untreated sample has main emission peaks at 617, 626 and 705 nm. As the annealing temperature increases, these emission lines lose strength, and new emission lines appear at 611, 631, 709 and 712 nm. This starts at a temperature of 950 °C. The 611 nm emission line quickly becomes the strongest. The unexpected appearance of an emission line at 702 nm was observed, but this disappears again at high annealing temperatures. The reason for this appearance is currently unclear and being investigated.
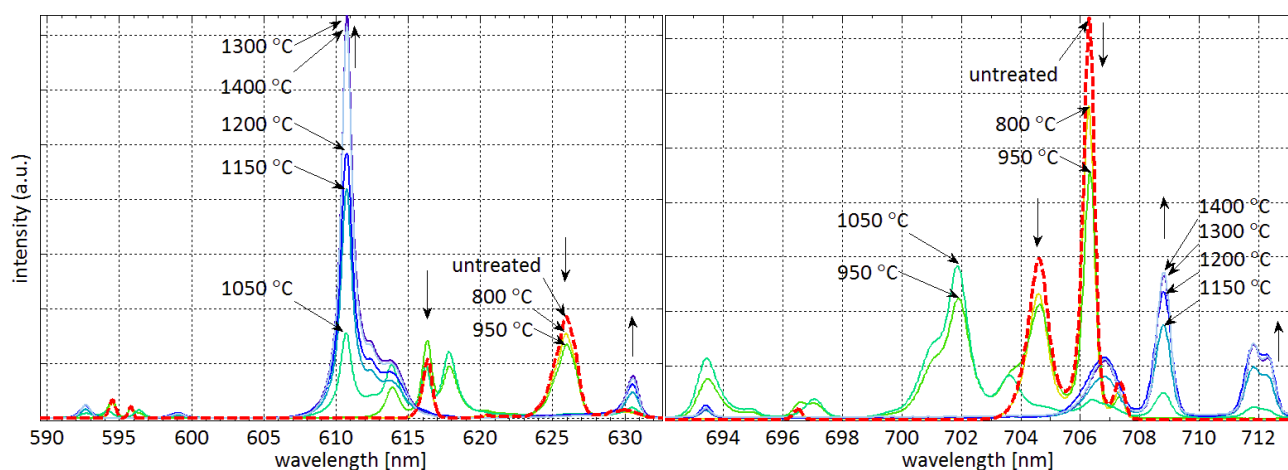

Figure 4: **Emission spectra of $Y_2O_2S : Eu$ samples at different annealing temperatures for 40 min, centered around 610 nm (left) and 705 nm (right). Excited at 266 nm**

Figure 5 shows the evolution of the peak emission intensity of major emission lines versus annealing temperature. The emission lines at 611, 630 and 705 nm increase in intensity for exposures of up to 1000 °C. The emission lines at 617 and 626 nm, which are the main emission lines of untreated $Y_2O_2S : Eu$, increase initially up to 1000 and 900 °C, respectively, before dropping to very small values. The rise in the emission intensity at 611 nm follows a quasi linear behaviour. This suggests that this phosphor can be used as phosphorescent thermal history sensor from 950 to 1300 °C using this emission line. Past 1300 °C, there seems to be some ambiguity in the response.

The emission spectra of untreated $Y_2O_2S : Eu$, $Y_2O_3 : Eu$ and annealed at 1400 °C $Y_2O_2S : Eu$ are shown in figure 6. The emission spectrum of the heat-treated sample looks very similar to the spectrum of $Y_2O_3 : Eu$. This indicates that the $Y_2O_2S : Eu$ looses sulfur when exposed to high temperatures, and this has a profound effect on the emission spectrum of the phosphor. It shows that the heat-treated $Y_2O_2S : Eu$ becomes $Y_2O_3 : Eu$. Commercial $Y_2O_2S : Eu$ is made by sulfurisation
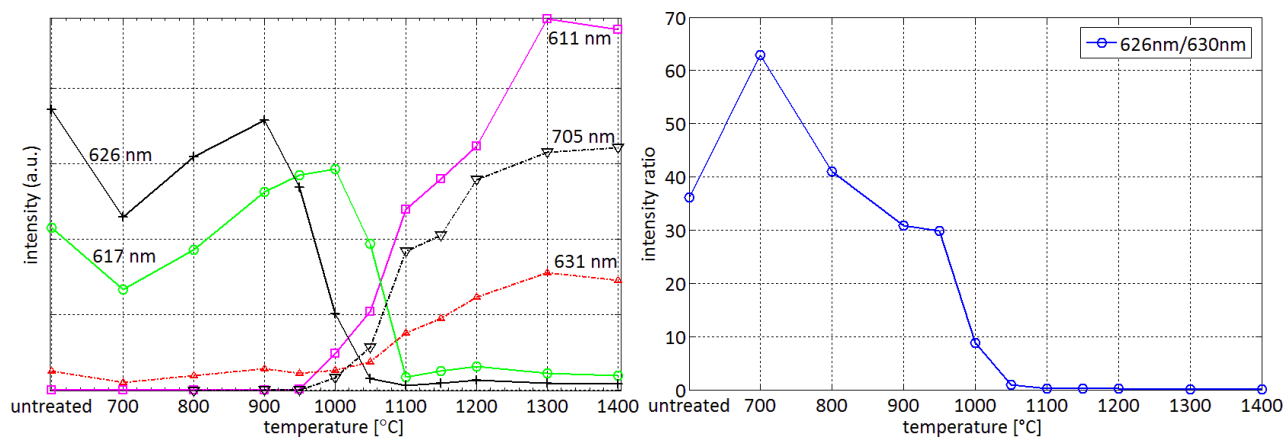
Figure 5: **Emission peak intensity of** $Y_2O_2S : Eu$ **samples at various major emission lines, at different annealing temperatures, for 40 min. Excited at 266 nm**

of $Y_2O_3 : Eu$ [Yen et al., 2007]. It is interesting to notice that the sulfurisation is reversed by exposing the phosphor to high temperatures in air.

Photoluminescent Lifetime Decays

Figure 7 ($left$) shows the lifetime obtained from fitting an exponential decay curve to the emission from $Y_2O_2S : Eu$ powder particles annealed at different temperatures for 20 and 40 min. The samples were excited at 266 nm. The lifetime of the annealed samples are compared to untreated $Y_2O_2S : Eu$. The errorbars are computed from 30 exposures per sample, and an average and standard deviation of the resulting 30 lifetimes is plotted. The lifetime of the phosphor samples annealed for 40 min, at both emission wavelengths, increases up to 1100 °C. One can observe that the lifetime at 630 nm needs higher temperatures to change.

When looking at the curves obtained from 20 min thermal exposure and excitation at 266 nm, we see that the 610 nm emission line follows the trend of the 610 nm decay curve at 40 min quite well. The lifetime changes less rapidly and reaches a saturation lifetime when exposed to higher temperatures. However, at 630 nm, the change is much weaker, and not monotonic at all. This
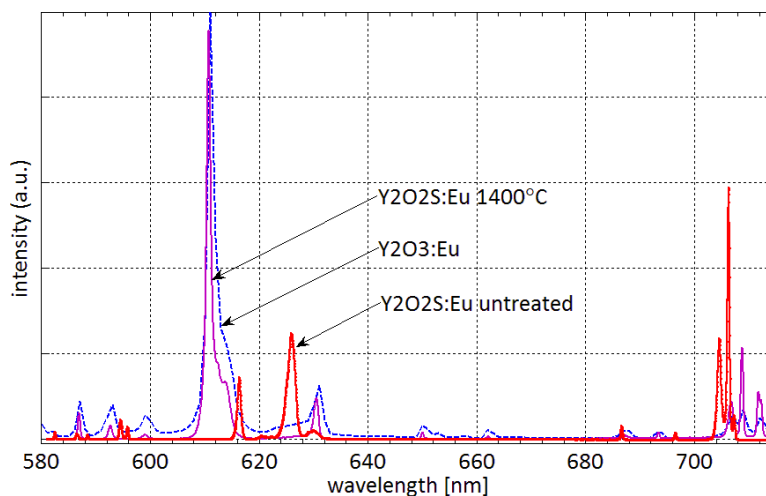

Figure 6: **Emission spectra of untreated** $Y_2O_2S : Eu$**,** $Y_2O_3 : Eu$ **and** $Y_2O_2S : Eu$ **heat-treated at 1400 °C. Excited at 266 nm**
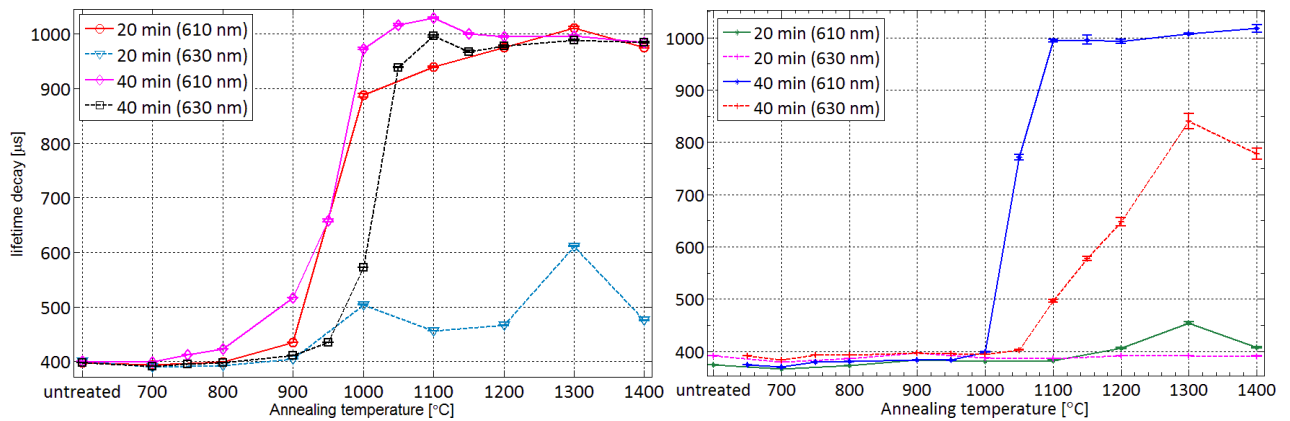
Figure 7: **Lifetime decay of the emission at 610 and 630 nm of $Y_2O_2S : Eu$ samples at different annealing temperatures. Samples were heat-treated for 20 and 40 min. Excited at 266 nm (left) and 355 nm (right)**

shows that this phosphor has an important time dependency. More research needs to be conducted to establish a potential thermal exposure time, after which the lifetime does not change.

Figure 7 ($right$) shows the lifetimes of the same samples, excited at 355 nm, in the CTS. The lifetime of the annealed samples are again compared to untreated $Y_2O_2S : Eu$. The lifetimes of the phosphor samples annealed for 40 min does not vary much up to 1000 and 1050 °C, for 610 and 630 nm respectively. At higher temperatures, a strong increase in the lifetime decay is observed at both emission lines. It is interesting to notice that the changes in lifetime are observed at a higher temperature than at 266 nm. The changes seem to affect the CTS in lesser manner than the host lattice. The samples exposed for 20 min barely show any change in lifetime with increasing annealing temperature. This indicates that the changes in the CTS need more thermal exposure to appear, contrarily to the changes in the host.

Sensitivity analysis

A initial sensitivity analysis was conducted on the phosphor samples. Figure 8 ($left$) shows a set of samples covering the temperature range between 950 and 1100 °C for 610 nm. A monotonic
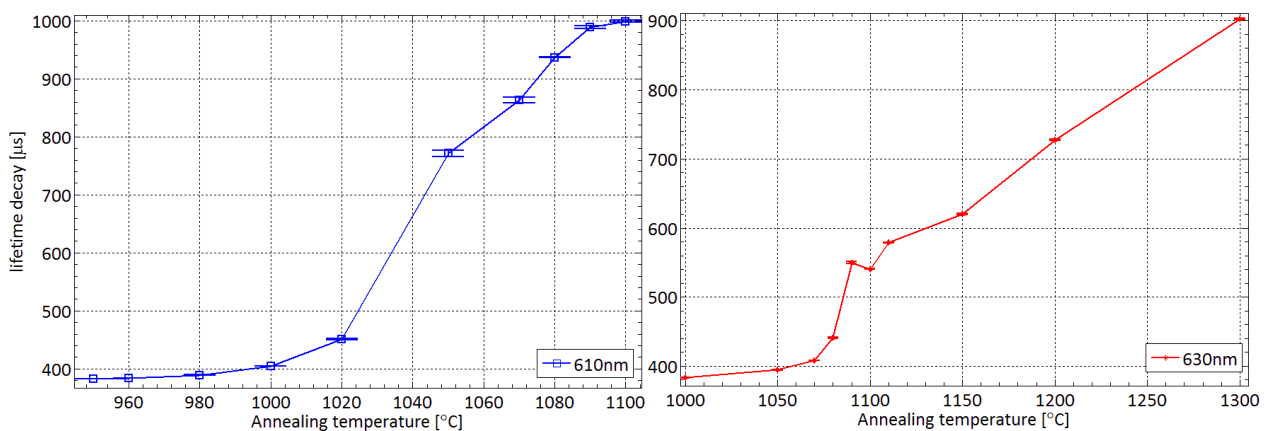

Figure 8: **Lifetime decay of the emission at 610 nm (left) and 630 nm (right) of $Y_2O_2S : Eu$ samples at different annealing temperatures. Samples were heat-treated for 40 min. Excited at 355 nm.**

increase of the lifetime decay for the 610 nm line is observed. The resolution over that ranges varies from 1 to 15 μs/°C and the error on the temperature varies from 1 to 3 °C. In Figure 8 ($right$), a set of samples covering the temperature range between 1000 and 1300 °C for 630 nm is plotted. A quasi monotonic increase of the lifetime decay is observed for the 630 nm line. The resolution over that ranges varies from 0.3 to 4 μs/°C and the error on the temperature varies from 0.5 to 15 °C. These initial results require further confirmation and work is currently in progress.

CONCLUSIONS AND OUTLOOK

The concept for a new type of thermal history sensing paint based on phosphorescent materials has been introduced and the potential advantages of such a paint over conventional thermal paints have been discussed. Different processes giving rise to permanent emission changes have been presented. Experimental demonstration of the phase-change concept, using $Y_2O_2S : Eu$ was given. The samples were annealed at different temperatures for 20 and 40 min, excited at two frequencies and observed at two emission wavelengths.

Major emission lines in the spectrum of $Y_2O_2S : Eu$ disappeared with increasing annealing temperatures, while others, characteristic to $Y_2O_3 : Eu$ appeared. Some emission lines were found to increase or decrease in emission intensity in a quasi linear fashion. The lifetime measurements provided robust, intensity independent results. Strong increase in the lifetime decays were observed for samples heat-treated at temperatures past 900 °C. Using both excitation wavelengths, the phosphor is able to cover a temperature history range from 700 to 1400 °C. The results at 630 nm from samples annealed for 20 min are poor, compared to those annealed for 40 min. An initial error approximation indicates that the error on the temperature in the dynamic range of the phosphor varies from 1 to 15 °C.

Other thermal exposure times have not been investigated, but more work is ongoing to investigate in more detail the dependency of the changes with time and temperature. A more comprehensive calibration of the phosphor will be presented in due course. Phosphors that undergo permanent changes due to other processes than the phase-change process will be investigated. It is anticipated that other phosphors exhibiting a wider temperature dynamic range exist and further research to identify these is also underway. In a next step, the phosphor will be applied and tested as a paint on a metallic or ceramic substrate. Future issues that need to be addressed are the homogeneity and uniformity of the paint and the choice of the binder to which the amorphous phosphor will be added. Also, a stable, standard phosphor will be added to the phosphor and applied on a surface, and the intensity ratio will be calibrated against maximum exposure temperatures.

References

S.W. Allison and G.T. Gillies. Remote thermometry with thermographic phosphors: Instrumentation and applications. *Review of Scientific Instruments*, 68:2615, 1997.

C. Bird, J.E. Mutton, R. Shepherd, M.D.W. Smith, and H.M.L. Watson. Surface temperature measurement in turbines. *AGARD Conference Proceedings*, 598:21.4–21.10, 1998.

G. Blasse and B.C. Grabmaier. *Luminescent Materials*. Springer Verlag, 1994.

J. Brubach, J.P. Feist, and A. Dreizler. Characterization of manganese-activated magnesium flu-

orogermanate with regards to thermographic phosphor thermometry. *Measurement Science and Technology*, 19(2):25602, 2008.

MD Chambers and DR Clarke. Terbium as an alternative for luminescence sensing of temperature of thermal barrier coating materials. *Surface and Coatings Technology*, 202(4-7):688–692, 2007.

JE Cowling, P. King, and A.L. Alexander. Temperature-indicating paints. *Industrial & Engineering Chemistry*, 45(10):2317–2320, 1953.

G.H. Dieke, H.M. Crosswhite, and H. Crosswhite. *Spectra and energy levels of rare earth ions in crystals*. Interscience Publishers, 1968.

G.E. Fair, R.J. Kerans, and T.A. Parthasarathy. Thermal history sensor based on glass-ceramics. *Sensors and Actuators: A. Physical*, 141(2):245–255, 2008.

J. Feist, J. Nicholls, and A. Heyes. Determining thermal history of components. (inventors), 2007. Patent WO/2009/083,729.

J.P. Feist and A.L. Heyes. The characterization of $Y_2O_2S : Sm$ powder as a thermographic phosphor for high temperature applications. *Measurement Science and Technology*, 11(7):942–7, 2000.

J.P. Feist and A.L. Heyes. Smart tbc's for gas turbines. *International Society for Air Breathing Engines*, Bangalore, India, 2001.

J.P. Feist, A.L. Heyes, K.L. Choy, and B. Su. Phosphor thermometry for high temperature gas turbine applications. In *Instrumentation in Aerospace Simulation Facilities*, page 6, 1999.

W.H. Fonger and C.W. Struck. Eu^{3+} ^5D resonance quenching to charge-transfer states in Y_2O_2S, La_2O_2S, and $LaOCl$. *J. Chem. Phys*, 52(12):6364–6372, 1970.

A.L. Heyes, J.P. Feist, X. Chen, Z. Mutasim, and J.R. Nicholls. Optical nondestructive condition monitoring of thermal barrier coatings. *Journal of Engineering for Gas Turbines and Power*, 130: 0613011–0613018, 2008.

C. Lempereur, R. Andral, and J.Y. Prudhomme. Surface temperature measurement on engine components by means of irreversible thermal coatings. *Measurement Science and Technology*, 19(10): 105501, 2008.

A.J. Neely and W.C. Tjong. Calibration of thermal paints for hypersonic flight test. *AIAA 2008*, page 2664, 2008.

V.A. Nikolaenko, V.A. Morozov, and N.I. Kasianov. A crystal maximum temperature measure (imtk) for special application. *Rev/ int Htes Temp. Et Refract*, 13:17–20, 1976.

J.A. Poston, R.V. Siriwardane, E.P. Fisher, and A.L. Miltz. Thermal decomposition of the rare earth sulfates of cerium (III), cerium (IV), lanthanum (III) and samarium (III). *Applied Surface Science*, 214(1-4):83–102, 2003.

A. Rabhiou, A. Kempf, and AL Heyes. Examination of Eu-doped thermographic phosphors for surface temperature measurements. In *European Combustion Meeting, Vienna, Austria*, 2009.

No 1907/2006 Regulation EC. Registration, evaluation, authorisation and restriction of chemicals. *Journal ref: L396, 30 ,pp.1-849*, 12.2006.

R.R. Rolls-Royce. Temperature indicative paint, 1988. UK Patent GB2204874.

M.D.W. Smith. Interpretation of thermal paint. (inventor), 2002. Patent US 6/434,267.

R.J.L. Steenbakker, J.P. Feist, R.G. Wellman, and J.R. Nicholls. Sensor thermal barrier coatings: Remote in situ condition monitoring of EB-PVD coatings at elevated temperatures. *Journal of Engineering for Gas Turbines and Power*, 131:041301, 2009.

A.A. Volinsky, VA Nikolaenko, VA Morozov, and VP Timoshenko. Irradiated single crystals for high temperature measurements in space applications. In *Materials for Space Applications*, volume 1, page 3, 2005.

H.M.L. Watson and E.C. Hodgkinson. Temperature indicating paint. (inventors), 2002. Patent US 10/229,002.

H.M.L. Watson and E.C. Hodgkinson. Temperature indicative paint. (inventors), 2003. Patent US 0044987 A1.

W.M. Yen, S. Shionoya, and H. Yamamoto. *Phosphor handbook*. CRC Press, Boca Raton, FL, 2007.

J. Zhang, Z. Tang, Z. Zhang, W. Fu, J. Wang, and Y. Lin. Synthesis of nanometer Y_2O_3: Eu phosphor and its luminescence property. *Materials Science and Engineering A*, 334(1-2):246–249, 2002.

Y.H. Zhou and J. Lin. Morphology control and luminescence properties of YVO_4: Eu phosphors prepared by spray pyrolysis. *Optical Materials*, 27(8):1426–1432, 2005.

Y.H. Zhou, J. Lin, S.B. Wang, and H.J. Zhang. Preparation of $Y_3Al_5O_{12}$: Eu phosphors by citric-gel method and their luminescent properties. *Optical Materials*, 20(1):13–20, 2002.